

## 12B.6 ENVIRONMENTAL AND SIGNAL PROCESSING CONDITIONS THAT NEGATIVELY IMPACT THE PERFORMANCE OF THE WSR-88D TORNADO DETECTION ALGORITHM

W. David Zittel<sup>1\*</sup>, Robert R. Lee<sup>1</sup>, E. DeWayne Mitchell<sup>2</sup>, and Dale Sirmans<sup>1</sup>

<sup>1</sup>NEXRAD Radar Operations Center, Norman, Oklahoma

<sup>2</sup>National Severe Storms Laboratory/CIMMS, Norman, Oklahoma

### 1. INTRODUCTION

In 1997, the Radar Operations Center (ROC)--formerly WSR-88D Operational Support Facility--fielded a new algorithm to detect tornadic circulations as part of its Build 10 software release. This new algorithm, the Tornado Detection Algorithm (TDA), has a Probability of Detection (POD) of 43%, a False Alarm Ratio (FAR) of 48%, and a Critical Success Index (CSI) of 31% (Mitchell et al., 1998). The verification statistics are computed using a time-window scoring procedure developed at the National Severe Storms Laboratory (NSSL) by Witt et al., 1998. By contrast, the Tornado Vortex Signature (TVS) algorithm, that the TDA replaced, had a POD of 3%, an FAR of 0%, and a CSI of 3% (Mitchell et al., 1998). Although the TDA has a considerably improved POD, it also has a much higher FAR.

After 10 years of experience studying level II data from WSR-88D radars and evaluating algorithm performance, algorithm developers have come to classify TDA false alarm errors into two different types. Errors that arise from a combination of meteorological and signal processing conditions are called Type I false alarms; errors associated with bona fide regions of shear erroneously classified as tornadic are called Type II false alarms. The Build 10 TDA has been observed to generate both false alarm types.

Type I false alarms result from contaminated velocity estimates due to receiver saturation or clutter targets not removed by clutter suppression adjacent to meteorological targets. A change to the Velocity Dealiasing Algorithm (VDA) to support the new TDA allows many of the Type I false alarms to be retained within the velocity data.

In this paper we focus on Type I false alarms. Our purpose is to show that, with awareness of the source of the false alarms, we can allay concerns about using this algorithm operationally and suggest ways to mitigate false alarms.

### 2. TDA OVERVIEW

Processing by the TDA consists of multiple steps using both base velocity and reflectivity data from all available elevation slices within a volume coverage pattern. The algorithm identifies pairs of radially adjacent sample volumes, i.e., one-dimensional (1D) features, whose velocity difference exceeds a minimum threshold, nominally  $11 \text{ ms}^{-1}$ . Sample volumes must also have a corresponding user-selectable minimum reflectivity value, nominally 0 dBZ. The 1D features are further constrained to be within 100 km range of the radar and less than 10 km elevation above the radar height. Both constraints are adaptable. Next, two-dimensional (2D) features are formed by combining 1D features. If a potential 2D feature's radial extent divided by its azimuthal extent is below a threshold value and the feature does not overlap any other 2D features, the potential feature is saved. The 2D features from adjacent elevation scans are vertically correlated into potential three-dimensional (3D) features. Lastly, each 3D feature is compared against base height, elevation angle, and strength thresholds to determine if the feature is classified as an Elevated Tornado Vortex Signature (ETVS) or a Tornado Vortex Signature (TVS). It must be understood the TDA rarely detects tornado scale circulations due to beam broadening with range. The adaptable parameter settings used

in the cases below are the default set used in the WSR-88D. Additional details about algorithm processing can be found in Mitchell et al., 1998.

### 3. ANALYSIS

Level II Archive data were played back using the WSR-88D Algorithm Test and Display System (WATADS) developed by the NSSL (NSSL, 1999). WATADS contains both a suite of WSR-88D meteorological algorithms and a suite of experimental algorithms under development by the NSSL. Besides processing data through algorithms, WATADS provides a means of displaying base data products and overlaying algorithm output similar to the WSR-88D Principal User Processor system. It should be noted that the WSR-88D algorithms in WATADS perform very similarly to the operational WSR-88D algorithms but may not always produce identical results.

#### 3.1 Case 1 - Receiver saturation

On May 30, 1998, an F4 tornado struck the community of Spencer SD killing six people. Although the event preceded fielding of the TDA by several months, the ROC acquired a copy of Level II Archive data for testing the TDA. The data were collected by the Sioux Falls SD WSR-88D (KFSD) located about 70 km east-southeast of Spencer. Meteorological conditions were favorable for initiating severe storms this day (Service Assessment Report, 1998), and the storm that struck Spencer was just one of several storms. Separating TDA false alarms from valid TVSs during this event could be particularly troublesome for forecasters. We note there were both Type I and Type II false alarms on this day, but we will focus on the former.

As the storms approach within 48 km of the radar, the TDA begins to trigger multiple false alarms of first ETVSs and then TVSs.

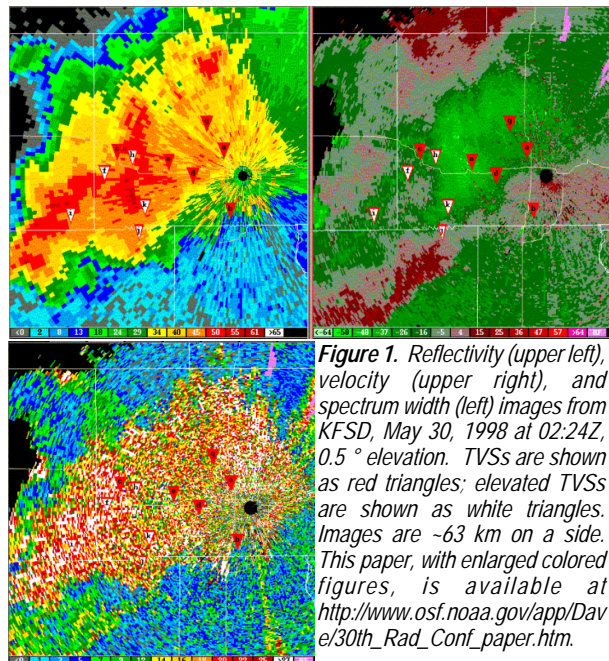


**Figure 1.** Reflectivity (upper left), velocity (upper right), and spectrum width (left) images from KFSD, May 30, 1998 at 02:24Z, 0.5° elevation. TVSs are shown as red triangles; elevated TVSs are shown as white triangles. Images are -63 km on a side. This paper, with enlarged colored figures, is available at [http://www.osf.noaa.gov/app/Dave/30th\\_Rad\\_Conf\\_paper.htm](http://www.osf.noaa.gov/app/Dave/30th_Rad_Conf_paper.htm).

\*Corresponding author address: W. David Zittel, WSR-88D ROC, 1200 Westheimer Dr., Norman, OK 73069; e-mail: Walter.D.Zittel@noaa.gov.

Figure 1 shows the reflectivity, velocity, and spectrum width data at 0.5 deg elevation at 02:34Z with the ETVS and TVS detections from this volume scan overlaid. The velocity data do not indicate any organized circulations, yet TVSSs and ETVSSs appear to be randomly distributed over all areas of the storm. The regions of high reflectivity (>40 dBZ) are correlated with areas of high spectrum width where normally we would expect uniformly low values in areas of descending, rain-cooled air. High spectrum width values are normally found along updraft/downdraft boundaries and around highly turbulent phenomena such as tornadoes. The cause of the anomalous TVSSs, we believe, is the saturation of the WSR-88D receiver as discussed in more detail in Section 4.1.

### 3.2 Case 2 - Moving clutter targets

KMTX, the WSR-88D for the Salt Lake City (SLC) National Weather Service Forecast Office is situated on a peninsula jutting into the Great Salt Lake at an altitude of 2.0 km MSL or about 0.7 km above the level of the lake. A Southern Pacific railway crosses the Great Salt Lake passing through the town of Lakeside on the west side of the lake, past the southern tip of the peninsula, and eastward to Ogden, UT. Through antenna sidelobes, the radar has an unobstructed view of the railway out to 56 km and a broken view out to 112 km. On a number of occasions the SLC forecast office staff have observed TVSSs associated with trains (Vasiloff, 1999). On October 13, 2000, the SLC forecast office observed false alarm TVSSs in a benign stratiform precipitation weather situation. Figure 2 shows a schematic of the Great Salt Lake area upon which two false alarm TVSSs and seven gate-to-gate shear positions for volumes between 12:47Z and 13:35Z have been superimposed. Note in particular how well the TVSSs align with the railway. One train is first identified at 12:47Z and moves westward. A second train, identified at 13:29Z, is also moving westward.

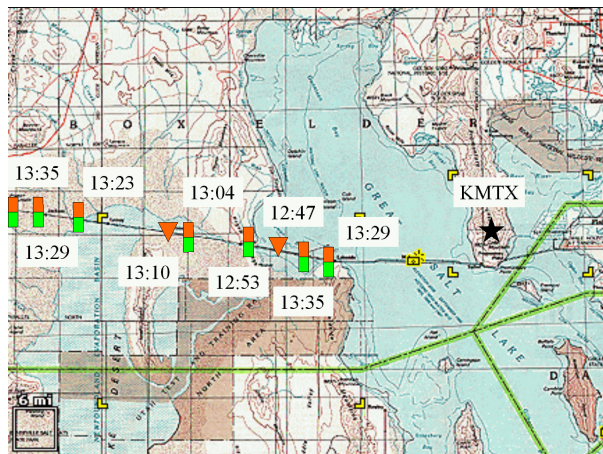


**Figure 2.** Schematic of Great Salt Lake area. Superimposed over the Southern Pacific Railway are TVSSs (red inverted triangles) and positions of gate-to-gate shear (red over green boxes) for October 13, 2000. Times are listed above or below the corresponding feature. KMTX radar location is shown as a black star. Area of map is ~125 km east/west and ~105 km north/south.

### 3.3 Case 3 - Weather & Sidelobe Contamination

On 15 January, 1999, Gray ME experienced a freezing rain event. The 12Z sounding indicated temperatures about -15C at the surface warming to 1C about 875 hpa. Winds were light from the northeast at the surface and veered with height to a southwesterly direction above the inversion with a speed in excess of 25 ms<sup>-1</sup>. Over the next twelve hours warm air advection weakened the inversion as

the surface flow became more southerly. During a three-hour period from ~17:40Z to ~20:40Z there were 28 TVS false alarms. The reflectivity data had isolated showers as high as 50 dBZ, probably due to bright-band contamination. The depth of the high reflectivity was only about one km. Figure 3 is a four-panel image at 19:46Z that shows a portion of reflectivity and velocity fields at 2.4° and 3.4° with two TVSSs overlaid. The weak reflectivity signal suggested the primary radar beam was not being refracted toward the ground. However, there were areas of near-zero velocities that induced the false alarms. The moderate spectrum width values (not shown) do not suggest problems with receiver saturation as with the Spencer SD case. We conclude that clutter coupling through side lobes may be causing the near-zero velocities.

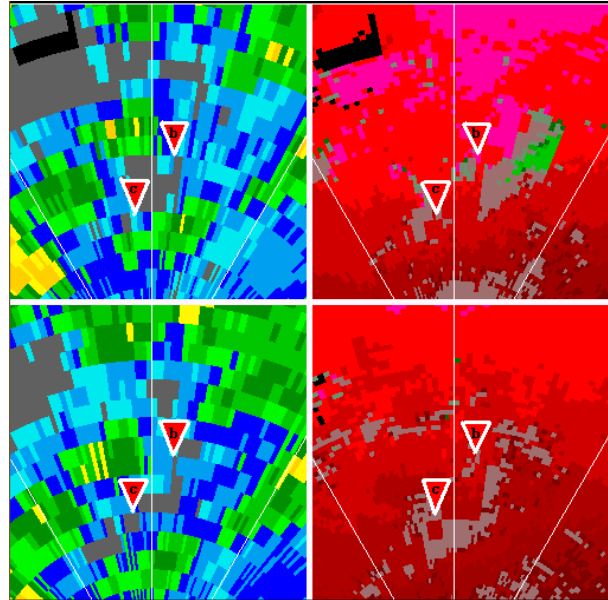


**Figure 3.** Reflectivity images (left) and velocity images (right) at 2.4° elevation (bottom) and 3.4° elevation (top) from the Gray, ME WSR-88D (KGYX) January 15, 1999 at 19:46Z. Type I false alarm TVSSs are shown as red triangles. Each image is ~16 km on a side.

Table 1 shows the 3D structure of the TVSSs. The lowest elevation for either TVS was 2.4°. Although the individual 2D features for TVS #1 show considerable positional change azimuthally, the cyclonic rotation signature visible in Figure 3 at 15°/15 km at the 3.4° elevation to the right of the TVSSs does not appear in Table 1 as one would expect.

Elev. (deg)	TVS #1			TVS #2		
	Azim. (deg)	Range (km)	Height (km)	Azim. (deg)	Range (km)	Height (deg)
2.4	4.8	13.9	0.6	355.3	10.8	0.5
3.4	5.3	12.9	0.8	353.5	9.8	0.6
4.3	10.5	12.0	0.9	346.6	9.9	0.7
6.0	13.8	10.0	1.1	345.1	11.1	1.2
9.9	21.3	10.9	1.9	349.6	10.7	1.8
14.6	-	-	-	347.1	12.4	3.1
19.5	26.9	12.9	4.3	354.6	11.0	3.7

**Table 1.** Location of 2D features for TVSSs shown in Figure 3.

## 4. MITIGATING FALSE ALARMS

### 4.1 Signal Processing

a) **Receiver Saturation.** The WSR-88D achieves a large receiver dynamic range (>90 db) by use of an "instantaneous" automatic gain control (AGC). The received signal is maintained in the linear region of the analog to digital converter by attenuating the signal. Attenuation is applied when the input signal exceeds a threshold equal to 60% of the analog-to-digital converter range and is of sufficient magnitude to "level" the signal to a constant value less than the converter maximum range. Setting of this AGC threshold is part of the receiver alignment procedure. Occasionally, due either to component drift or improper setup, the threshold is too high allowing the analog to digital converter to saturate before the AGC is activated. This limiting of the Doppler signal results in a severe distortion of the signal, which is manifested as an increase in signal spectrum width (by at least a factor of two) and generation of odd harmonics of the signal frequency. Under this condition, data quality is compromised caused by the large bias in width estimates, the corresponding increase in variance of the mean velocity estimates, and degraded clutter suppression due to the large width. A significant spectrum width-reflectivity correlation such as seen in Figure 1 should be cause for concern and possible initiation of a radar maintenance action. Receiver saturation monitoring and alarm generation will be incorporated in the WSR-88D Open Systems Radar Data Acquisition processor scheduled for fielding in a few years.

b) **Clutter Suppression.** The clutter suppression can compromise data quality in the presence of signal limiting or due to an improper filter setup. Some indications are removal of signals along the zero isodop and bias of velocities at or near the filter passband edge velocity. Signal removal can be detected in the base data display but the velocity bias cannot. Avoiding use of the "high" suppression when possible will mitigate clutter suppression impacts on data quality.

c) **Target Detection Through Antenna Side Lobes.** The WSR-88D has a respectable antenna pattern in terms of side lobe level. However, the overall system performance is such that even at several degrees off bore sight, where the two-way isolation is greater than 60 db, strong targets can be detected. Confined moving targets such as the train at Salt Lake City and vehicle traffic along highways are usually not difficult to identify. Further reduction of the antenna side lobe level does not appear practical and removal of these anomalous targets will require specialized signal processing. Stationary targets capable of side-lobe detection are also not difficult to identify. But again, specialized signal processing is required for removal. Use of high rather than moderate clutter suppression is usually of little benefit since the return signal-to-noise ratio exceeds the filter notch depth.

### 4.2 Algorithm Adaptable Parameters

Meteorological algorithms in the WSR-88D system use adaptable parameters that allow the performance to be fine-tuned for specific types of weather situations. Of the 30 adaptable parameters in the TDA only a few may be adjusted by users operationally. One adaptable parameter that may be adjusted is the reflectivity threshold used to filter the velocity data. In a study of a severe weather case, a subset of Mitchell et al. 1998, with bona fide TVSSs, Lester and Zittel (1997) found no change in the CSI (0.43) when the reflectivity threshold was raised from its default value of 0 dBZ to 10 dBZ and only a slight lowering of the POD (0.60 vice 0.63). The reflectivity threshold for TDA defaults to 0 dBZ. However, a forecaster observing TVSSs in weak reflectivity near the radar and in a weather regime where tornadoes are highly unlikely could raise the reflectivity threshold to reduce false alarms.

Another algorithm that affects the performance of the TDA is the Velocity Dealiasing Algorithm (VDA). Eilts and Smith (1990) found that they could greatly reduce velocity dealiasing errors if they allowed the algorithm to omit individual velocity bins that did not fit the surrounding

pattern. (The algorithm, as originally fielded, allowed up to four consecutive bins to be omitted before it replaced them.) However, valid TVSSs can be lost by removing velocity bins. With the fielding of the TDA, the VDA was modified to replace all omitted velocity bins but without compromising VDA performance. This change ensures TVSSs are identified but also allows high gate-to-gate velocity differences to exist in the velocity data, especially near the radar where ground clutter can introduce velocity bias and false gate-to-gate differences.

For the Gray ME case, raising the reflectivity threshold site adaptable parameter from the default value of 0 dB to 10 db eliminated 89% (25 / 28) of the TVS false alarms. When the VDA was allowed to omit velocity bins, the TDA again only generated three false alarms. Combining the two approaches eliminated all but one false alarm which occurred in a region of 24 dBZ echo.

## 5. SUMMARY

In this paper we have shown conditions under which the TDA will trigger Type I false alarms. Careful examination of the three base moments--reflectivity, velocity, and spectrum width--can indicate the cause of the false alarms. TVSSs that lie in areas of high spectrum width values that are also spatially correlated to moderate to high reflectivity (> 40 dBZ) may indicate receiver calibration problems. Remedial actions to re-calibrate the receiver will eliminate some false alarms.

Extended moving targets such as trains, especially when passing a hard stationary clutter target and isolated showers passing near a radar may, in the presence of side-lobe contamination, induce false alarms. Temporarily changing selected adaptable parameters in the TDA and VDA can mitigate these false detections. By understanding the effects of receiver saturation, moving clutter targets, side lobe contamination, and, most importantly, by using situational awareness, TDA users can successfully classify some ETVS / TVS detections as false alarms.

## 6. ACKNOWLEDGMENTS

The authors thank the many reviewers who provided suggestions for improving the paper and Krishna Rameeneedi, our webmaster.

## 7. REFERENCES

- Eilts, Michael D. and Steven D. Smith, 1990: Efficient dealiasing of Doppler velocities using local environmental constraints. *J. Atmos. Oceanic Technol.*, **7**, 118-128.
- Lester, Sarah I. and W. David Zittel, 1997: NSSL tornado detection algorithm reflectivity sensitivity testing, Preprints, *28<sup>th</sup> Conf. on Radar Meteorology*, Austin, Texas, Amer. Meteor. Soc., 359-360.
- Mitchell, E.D., S.V. Vasiloff, G.J. Stumpf, A. Witt, M.D. Eilts, J.T. Johnson, and K.W. Thomas, 1998: The National Severe Storms Laboratory tornado detection algorithm. *Wea. Forecasting*, **13**, 352 - 360.
- NSSL, 1999: WATADS (WSR-88D Algorithm Testing and Display System) version 10.2 Documentation. [Available at <http://www.nssl.noaa.gov/~watads/10doc.html>].
- Service Assessment Report: Spencer, South Dakota, Tornado, May 30, 1998.
- Vasiloff, Steven, 1999: The Utah West Desert Train Tornado. Western Region Technical Attachment No. 99-27, WRH/SSD. [available at <http://www.wrh.noaa.gov/>].
- Witt, A., M.D. Eilts, G.J. Stumpf, E.D. Mitchell, J.T. Johnson, and K.W. Thomas, 1998: Evaluating the Performance of WSR-88D Severe Storm Detection Algorithms. *Wea. Forecasting*, **13**, 513-518.
- WSR-88D Operational Support Facility, 1995: Anomalous target on Salt Lake City WSR-88D. Response to request for technical information number 13343. WSR-88D OSF, Norman, OK.